European Journal of Cardio-Thoracic Surgery 59 (2021) 1295–1303
doi:10.1093/ejcts/ezaa457 Advance Access publication 18 December 2020

ORIGINAL ARTICLE

Cite this article as: Zhao M, Deng J, Wang T, Li Y, Wu J, Zhong Y *et al.* Impact of computed tomography window settings on clinical T classifications and prognostic evaluation of patients with subsolid nodules. Eur J Cardiothorac Surg 2021;59:1295–303.

Impact of computed tomography window settings on clinical T classifications and prognostic evaluation of patients with subsolid nodules

Mengmeng Zhao[a,†], Jiajun Deng[a,†], Tingting Wang[b], Yingze Li[a], Junqi Wu[a], Yifang Zhong[a], Xiwen Sun[b], Gening Jiang[a], Yunlang She[a], Yuming Zhu[a], Dong Xie[a,*,‡] and Chang Chen[a,*,‡]

[a] Department of Thoracic Surgery, Shanghai Pulmonary Hospital, Tongji University School of Medicine, Shanghai, People's Republic of China
[b] Department of Radiology, Shanghai Pulmonary Hospital, Tongji University School of Medicine, Shanghai, People's Republic of China

* Corresponding author. Chang Chen, Department of Thoracic Surgery, Shanghai Pulmonary Hospital, Tongji University School of Medicine, Shanghai, 200443, China. Tel: (+86)13816869003; e-mail: chenthoracic@163.com (C. Chen); Tel: (+86)13918918907, e-mail: kongduxd@163.com (D. Xie).

Received 17 July 2020; received in revised form 3 November 2020; accepted 15 November 2020

Key question

What is the impact of CT display window settings on the clinical tumour (T) classifications and prognostic evaluation of subsolid nodules (SSNs)?

Key finding(s)

The use of the mediastinal window setting led to T classification shifts, but it did not affect SSN prognosis.

Take-home message

The current use of the lung window setting for determining clinical T classification and prognosis is appropriate as it stands.

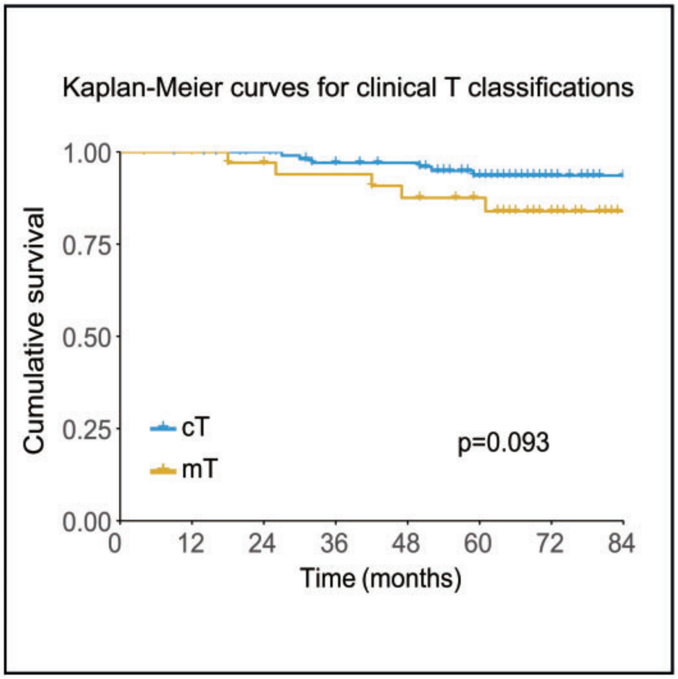

Abstract

OBJECTIVES: To investigate the impact of lung window (LW) and mediastinal window (MW) settings on the clinical T classifications and prognostic prediction of patients with subsolid nodules.

METHODS: Seven hundred and nineteen surgically resected subsolid nodules were reviewed, grouping into pure ground-glass nodules ($n = 179$) or part-solid nodules ($n = 540$) using LW. Interobserver agreement on nodule classifications was assessed via kappa-value, and predictive performance of the solid portion measurement in LW and MW for pathological invasiveness and malignancy were compared using receiver-operating characteristic analysis. Cox regression was used to identify prognostic factors. Prognostic significance of T

†The first two authors contributed equally to this work.
‡The last two authors contributed equally to this work as co-corresponding authors.
Accepted for presentation at the European Society of Thoracic Surgeons Annual Meeting 2020.

THORACIC

classifications based on LW (c[l]T) and MW (c[m]T) was evaluated by Kaplan–Meier method after propensity score matching. The performance of c(m)T for discrimination survival was estimated via the concordance index (C-index), net reclassification improvement and integrated-discrimination improvement.

RESULTS: By adopting MW, 124 part-solid nodules were reclassified as pure ground-glass nodules, and interobserver agreement improved to 0.917 (95% confidence interval 0.888–0.946). The solid portion size under MW more strongly predicted pathological invasiveness ($P = 0.030$), but did not better predict pathological malignancy. For remaining 416 part-solid nodules, c(l)T and c(m)T were both independent risk factors. c(m)T led to T classifications shifts in 321 nodules (14 upstaged and 307 downstaged) with no significant prognostic difference existing between the shifted c(m)T and matching c(l)T group after propensity score matching. The corrected C-index was improved to 0.695 (0.620–1.000) when adopting c(m)T with no significant difference in net reclassification improvement ($P = 0.098$) and integrated-discrimination improvement ($P = 0.13$) analysis.

CONCLUSIONS: As there is no significant benefit provided by MW in evaluating clinical T classification and prognosis, the current usage of LW is appropriate for assessing subsolid nodules.

Keywords: Pulmonary subsolid nodules • Computed tomography window setting • T staging • Prognosis

ABBREVIATIONS

c(l)T	Clinical T classifications determined under the lung window setting
c(m)T	Modified T classifications determined under the mediastinal window setting
CI	Confidence interval
CT	Computed tomography
HR	Hazard ratio
IDI	Integrated discrimination improvement
LW	The lung window setting
MW	The mediastinal widow setting
NRI	Net reclassification improvement
pGGNs	Pure ground-glass nodules
PSNs	Part-solid nodules
RFS	Recurrence-free survival
SSNs	Subsolid nodules
VPI	Visceral pleural infiltration

INTRODUCTION

Pulmonary subsolid nodules (SSNs) are classified as either part-solid nodules (PSNs) when containing solid components observed in the lung window (LW) setting of chest computed tomography (CT), or pure ground-glass nodules (pGGNs) [1]. The presence of a solid component in SSNs is a critical factor for patient's survival because the likelihood of malignancy correlates strongly with both the solid component size and growth rate [2]. Additionally, it has been reported that the solid component size of PSNs measured in the LW is significantly associated with pathological invasiveness and the prognosis of non-small-cell lung cancer patients [3]. These studies, as a result, have prompted the latest revision of the clinical T classification system. In the current 8th edition of T categorization, clinical T stages of SSNs should be based exclusively on solid component measurement under LW [4].

Current investigations on the CT display window settings used for SSNs solid component measurements indicate considerable controversy. On the one hand, using the LW increases the sensitivity for the detection of solid components, which could remain undetected with the mediastinal window (MW) setting [5]. The solid size in the LW also yields results more closely related to pathological invasive size [6]. In addition, the recommendation of the Fleischner Society in 2017 supported the application of the LW for the solid size measurements of SSNs [7]. On the other hand, usage of the MW enables enhancement of the inter-reader agreement on SSNs classifications and measurements [8, 9]. Moreover, Samejima *et al.* [10] demonstrated that the pathological invasive size of clinical IA lung adenocarcinoma could be estimated more precisely by measuring the lesion size in the MW.

Additionally, there is currently only one study available that compares the prognostic impact of different CT displays on the clinical T classification regarding both part-solid and pure solid nodules [11]. Furthermore, the impact of CT display window settings on clinical T classification and prognostic evaluation, especially for SSNs, has not yet been identified and confirmed. Thus, the purpose of the present study is to evaluate the impact of the LW and MW on clinical T classification and prognostic prediction for patients with SSNs.

PATIENTS AND METHODS

Ethical statement

Institutional review board (IRB) approval and waivers of consent were obtained from Shanghai Pulmonary Hospital (number K20-003, 20 January 2020).

Study population

We retrospectively evaluated the medical records of patients with radiological SSNs who underwent complete resection at our centre from January 2011 to December 2014, and the detailed patient inclusion criteria are illustrated in Fig. 1. Recurrence-free survival (RFS) was calculated as the time from the date of surgery to the date of recurrence and the follow-up strategy is described in Supplementary Material, SI. All patients in the study completed follow-up until 31 October 2019.

Radiological and histological evaluation

The details are described in Supplementary Material, SII. All nodules' type was re-evaluated by 2 radiologists (T.W. and X.S. with 5 years and 30 years of experience in chest CT) by using the LW (width/level, 1600/-400 HU). Then, the radiologists were required to reclassify these nodules via the following criterion: if a solid component was detected in the MW (width/level, 450/10 HU),

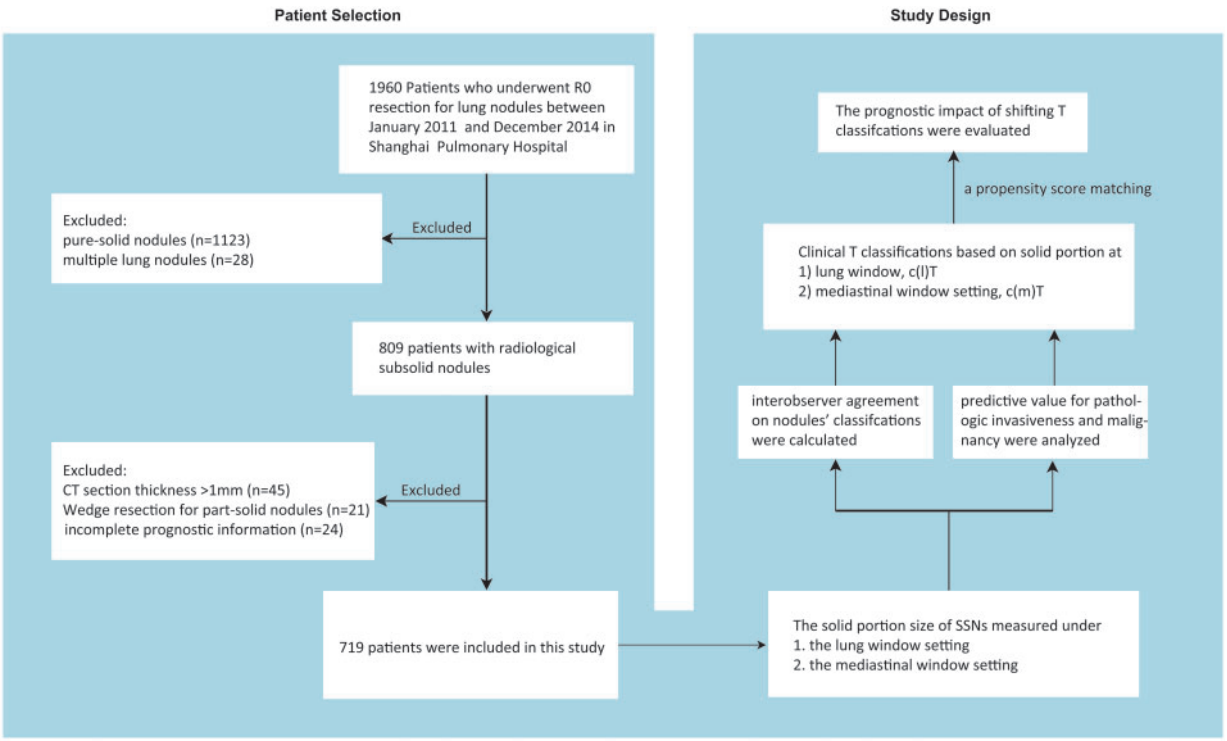

Figure 1: Flow chart of patient inclusion criteria and schematic representation of the study. c(l)T and c(m)T, clinical T classifications determined using the lung and mediastinal window settings; CT: computed tomography; SSNs: subsolid nodules.

the nodule was classified as a PSN; otherwise, it was classified as a pGGN (Fig. 2). The nodule size was determined by the average solid size measured by 2 radiologists. All the CT image reviewers were blinded to the patients' outcomes. SSNs were categorized as follows: Tis (solid portion size = 0 cm); Tmi (≤0.5 cm for part-solid); T1a (0.6–1 cm for part-solid); T1b (1–2 cm); T1c (2–3 cm); the T classifications was coded twice according to the solid portion size measured in the LW (c[l]T) and MW (c[m]T) [4].

Study design

As illustrated in Fig. 1, interobserver agreement on nodule classifications by using the LW and MW was calculated, and the predictive value of the solid portion size under LW and MW for pathological invasiveness and malignancy was compared. Then, the prognostic value of shifting T classification was investigated by performing propensity score matching for subgroups with no less than 10 patients [12]. Further, the additional prognostic value of c(m)T was also evaluated.

Statistical analysis

The patients' baseline characteristics were compared using Pearson's χ^2 test or Fisher's exact test for categorical variables when appropriate, and the independent *t*-test was used for continuous variables. Interobserver agreement was determined by calculating kappa statistics and considered poor (0.20), fair (0.21–0.40), moderate (0.41–0.60), good (0.61–0.80) or excellent (0.81–1.00) [13]. Receiver-operating characteristic (ROC) analyses were performed to compare the predictive values of the solid portion size measured in the LW and MW for pathological invasiveness and malignancy, including lymph node metastasis and visceral pleural invasion (VPI). Area under the ROC curve was compared via DeLong test. To identify the predictive factors for RFS of patients with 416 PSNs determined by the MW, univariable analysis was performed using Cox regression, whereas multivariable analysis was performed by the backward elimination method with a significance level <0.15. The complementary log–log plot model was used for the proportional hazards assumption. Because of notable imbalances in baseline covariates between the study groups, propensity score matching was conducted and is detailed in Supplementary Material, SIII. RFS curves were generated via the Kaplan–Meier method and compared by stratified log-rank test in the matched cohorts. Median follow-up time was calculated by reverse Kaplan–Meier survival.

The survival discrimination performances of clinical T classifications in the matched cohorts were evaluated by the corrected Harrell's concordance index (C-index) using bootstrap procedure. The additional discrimination value of c(m)T for prognosis was evaluated by net reclassification improvement (NRI) and integrated discrimination improvement (IDI). The *P*-values for NRI and IDI were calculated by Z statistics. Statistical analyses were conducted using SPSS 22.0 (IBM Corporation, Armonk, NY, USA) and R version 3.5.3 (http://www.R-project.org). An unadjusted 2-sided $P < 0.05$ indicates statistically significant difference.

RESULTS

Patient characteristics

Of all SSNs, 179 (24.9%) were classified as pGGNs and 540 (75.1%) were classified as PSNs via the LW. After adopting the MW, 303 (42.1%) nodules were classified as pGGNs, and the remaining 416

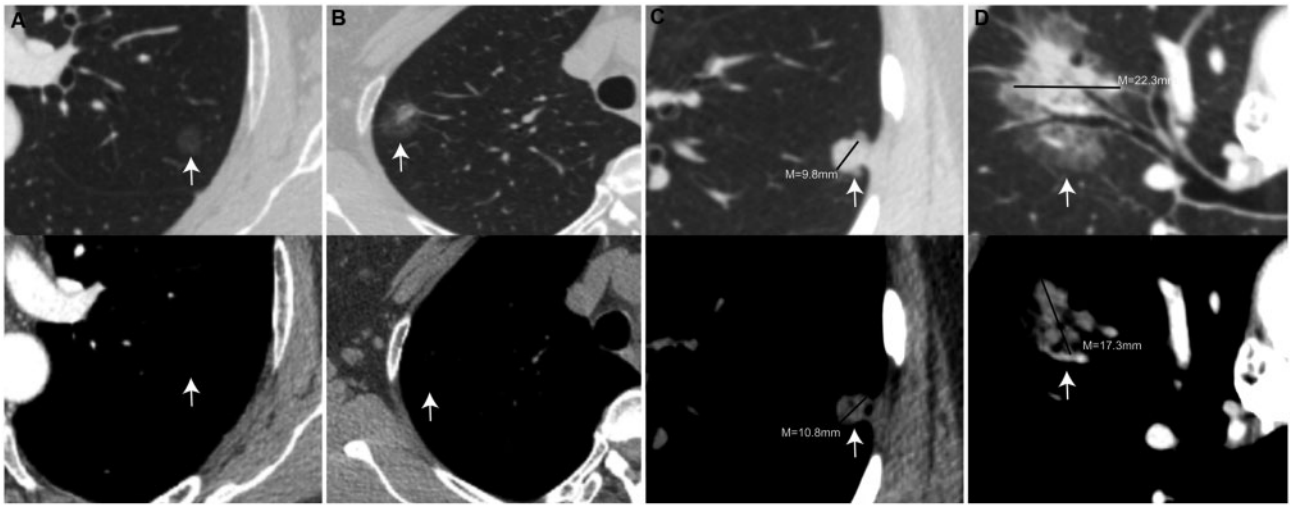

Figure 2: Comparison of the lung and mediastinal window images for subsolid nodules, including pure ground-glass nodules (**A**), part-solid nodules in the lung window without a solid portion (**B**), larger solid portion (**C**) or smaller solid portion in the mediastinal window (**D**). (**Top row**) Lung window image; (**bottom row**) mediastinal window image. The white arrow refers to the nodule included. M stands for the consolidation diameter.

Table 1: Clinicopathological characteristic of patients from pGGNs and PSNs group classified by lung and mediastinal window setting in this study

Characteristics	Under LW		Under MW	
	pGGNs (*n* = 179)	PSNs (*n* = 540)	PGGNs (*n* = 303)	PSNs (*n* = 416)
Age (years)				
<65	157 (87.7)	400 (74.1)	259 (85.5)	298 (71.6)
≥65	22 (12.3)	140 (25.9)	44 (14.5)	118 (28.4)
Sex				
Male	67 (37.4)	201 (37.2)	116 (38.3)	152 (36.5)
Female	112 (62.6)	339 (62.8)	187 (61.7)	264 (63.5)
LD (cm), mean ± SD	0	1.14 ± *0.69*	0	1.40 ± *0.67*
MD (cm), mean ± SD	0	0.75 ± *0.76*	0	1.03 ± *0.69*
Lesion side				
Left	66 (36.9)	215 (39.8)	120 (39.6)	161 (38.7)
Right	113 (63.1)	325 (60.2)	183 (60.4)	255 (61.3)
Surgery procedure				
Sublobar resection	49 (27.1)	46 (8.3)	72 (23.2)	23 (5.4)
Segmentectomy	10 (5.5)	32 (5.7)	25 (8.0)	17 (4.0)
Lobectomy	120 (66.3)	462 (82.6)	206 (66.2)	376 (87.6)
Histological subtype				
Adenocarcinoma				
AAH	19 (10.5)	5 (0.9)	24 (7.7)	
AIS	44 (24.6)	20 (3.7)	55 (18.2)	9 (2.2)
MIA	55 (30.7)	65 (12.0)	98 (32.3)	22 (5.3)
Invasive adenocarcinoma				
Lepidic	31 (17.3)	209 (38.7)	70 (23.1)	170 (40.9)
Acinar	25 (13.8)	152 (27.2)	42 (13.9)	135 (32.5)
Papillary	5 (2.8)	81 (15.0)	14 (4.6)	72 (17.)
Solid	0 (0)	8 (1.5)	0 (0)	8 (1.9)
Lymph node metastasis				
N0	179 (100)	533 (98.7)	303 (100)	409 (98.3)
N1/N2	0 (0)	7 (1.3)	0	7 (1.3)
VPI (presence)	5 (2.8)	34 (6.3)	6 (2.0)	33 (7.9)

Categorical data are shown as numbers (%).

AAH: atypical adenocarcinoma hyperplasia; AIS: adenocarcinoma *in situ*; LD: solid portion size measured at LW; LW: the lung window setting; MD: nodule size measured at MW; MIA: minimally invasive adenocarcinoma; MW: the mediastinal window setting; pGGNs: pure ground-glass nodules; PSNs: part-solid nodules; VPI: visceral pleural infiltration.

Table 2: Comparison of clinical characteristic between patients in the matched cohorts

Characteristics	Down-staged cases (n = 82)	Cases with no shifting cT (n = 82)	Standardized difference
Age (years)			0.86
<65	55 (67.1)	53 (64.6)	
≥65	27 (32.9)	29 (35.4)	
Sex			>0.99
Male	29 (35.4)	29 (35.4)	
Female	53 (64.6)	53 (64.6)	
LD (cm), mean ± *SD*	1.35 ± *0.59*	1.37 ± *0.65*	0.63
MD (cm), mean ± *SD*	0.99 ± *0.50*	1.00 ± *0.53*	0.62
Lesion side			>0.99
Left	30 (36.6)	29 (35.4)	
Right	52 (63.4)	53 (64.6)	
Surgery procedure			>0.99
Sublobar resection	9 (11.0)	10 (12.2)	
Lobectomy	73 (89.0)	72 (87.8)	
Histological subtype			0.057
Adenocarcinoma	4 (4.9)	12 (14.6)	
AIS	1 (1.2)	5 (6.1)	
MIA	3 (3.7)	7 (8.5)	
Invasive adenocarcinoma	78 (95.1)	70 (85.4)	
Lepidic	34 (41.5)	29 (35.4)	
Acinar	30 (36.6)	24 (29.3)	
Papillary	14 (17.1)	15 (18.3)	
Solid	0 (0)	2 (2.4)	
Lymph node metastasis			/
N0	82 (100)	82 (100)	
VPI (presence)	7 (8.5)	2 (2.4)	0.18

Categorical data are shown as numbers (%).
AIS: adenocarcinoma *in situ*; cT: clinical T classifications; LD: solid portion size measured at lung window setting; MD: nodule size measured at mediastinal window setting; MIA: minimally invasive adenocarcinoma; MW: the mediastinal window setting; VPI: visceral pleura infiltration.

(57.9%) nodules were PSNs. The baselines characteristics are summarized in Table 1. Interestingly, 124 (17.2%) PSNs were reclassified into the pGGNs group when applying the MW, of which 5 (0.7%) nodules pathologically confirmed as atypical adenomatous hyperplasia were correctly reclassified as pGGNs. No significant differences regarding age ($P = 0.19$), sex ($P = 0.71$), lesion side ($P = 0.24$) and VPI ($P = 0.22$) existed between the 124 pGGNs determined using the MW and 179 pGGNs determined using the LW (Supplementary Material, Table S1). The median follow-up time of all patients was 69.0 months (interquartile range, 61–75 months).

Recurrence occurred in 35 patients, and the 5-year RFS rate of all patients was 95.7% [95% confidence interval (CI) 0.941–0.973]. The 5-year RFS rates for the pGGNs and PSNs groups classified by the LW were 100% and 94.2% (95% CI 0.920–0.964; $P < 0.001$; Supplementary Material, Fig. S1A), respectively. The 5-year RFS rates for the pGGNs and PSNs groups classified by the MW were 100% and 92.4% (95% CI 0.897–0.951; $P < 0.001$; Supplementary Material, Fig. S1B). Propensity score matching generated 82 matched cases from the group without T classification shifting and 82 cases from the downstaged group with well-balanced baselines characteristics (Table 2).

Interobserver agreement on nodule classifications and pathological findings

The interobserver agreement regarding nodule classification was excellent in the MW (kappa: 0.917; 95% CI 0.888–0.946) and good (kappa: 0.773; 95% CI 0.722–0.824) in the LW. The area under the ROC curve of the solid portion size measured in the LW for predicting pathological invasiveness was 0.870 (95% CI 0.843–0.894), which is significantly higher than that for the solid portion size measured in the MW (area under the ROC curve: 0.848; 95% CI 0.820–0.874; $P = 0.030$; Fig. 3A). Moreover, lymph node metastasis and VPI were better predicted by the solid portion size measured in the MW (Fig. 3B–D).

Survival outcomes before propensity score matching

Both c(l)T and c(m)T significantly distinguished the prognosis of all patients in our study (Supplementary Material, Fig. S1), and no recurrence occurred in the c(m)Tis cases. The solid size measured in the MW led to clinical T classification shifts in 321 cases (Fig. 4). Upstaging occurred in 4.4% (14/321) of cases and downstaging occurred in 95.6% (307/321) of cases (Supplementary Material, Table S3). The 5-year RFS rate was 92.9% (95% CI 0.794–1.000) and 96.4% (95% CI 0.942–0.986) for upstaged and downstaged cases. The presence of upstage or downstage for T classifications had no prognostic value for patients with PSNs determined at the MW (Table 3). The prognostic value of c(l)T [T1b: hazard ratio (HR) 3.379; 95% CI 1.091–10.465; $P = 0.035$; T1c: HR 6.303; 95% CI 2.102–18.898; $P = 0.001$], and c(m)T (T1b: HR 3.304; 95% CI 1.380–7.911; $P = 0.007$; T1c: HR 4.202; 95% CI 1.671–10.565; $P = 0.002$) were still powerful in multivariable analysis.

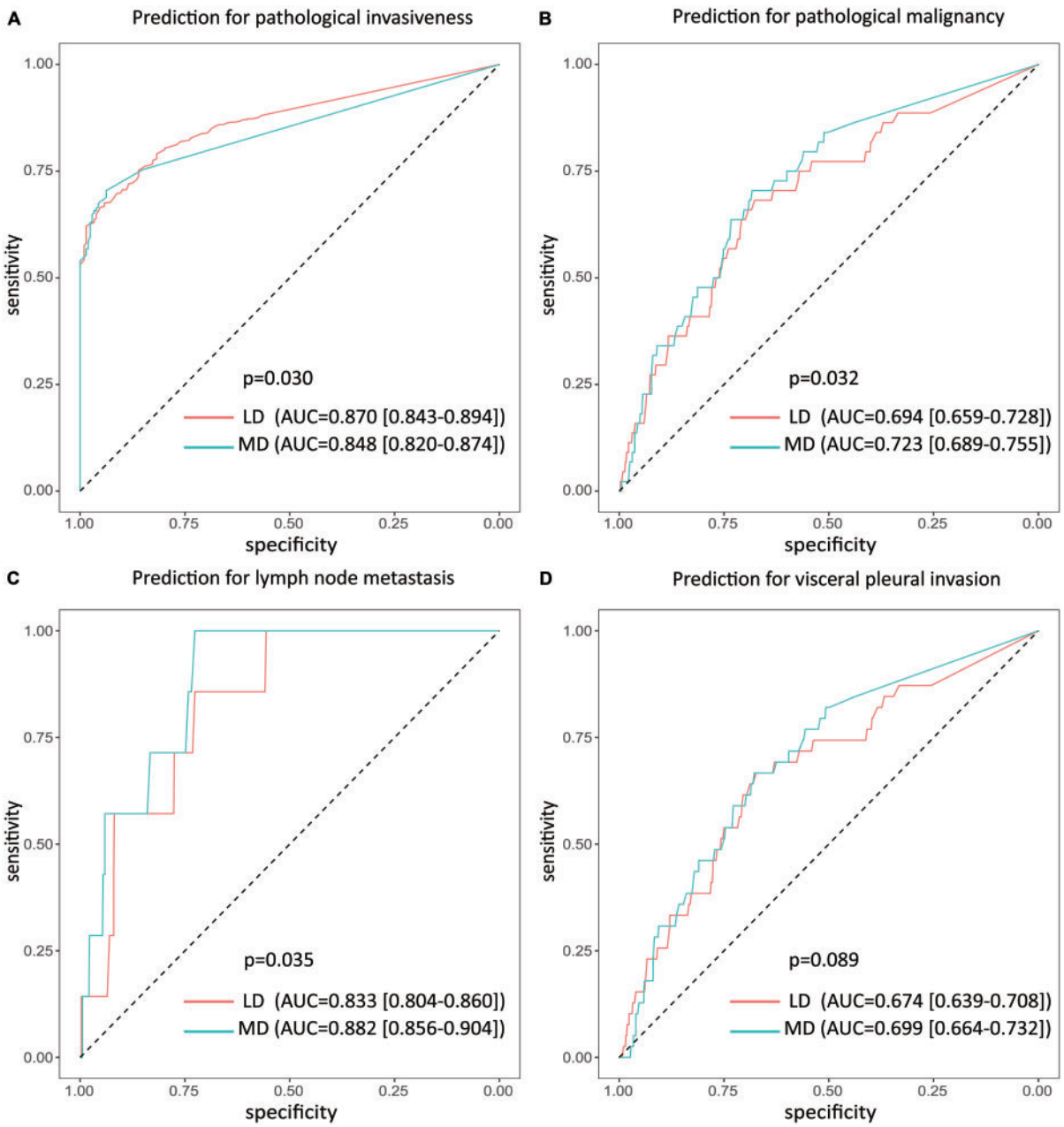

Figure 3: Receiver-operating characteristic curves of the predictive performance for (**A**) pathological invasiveness and (**B**) pathological malignancy, including (**C**) lymph node metastasis and (**D**) visceral pleural invasion. AUC, area under the receiver-operating characteristic curve; LD: the solid portion size with the lung window setting; MD: the solid portion size measured with the mediastinal widow setting.

Survival analysis in the matched cohorts

No recurrence occurred in Tmi groups. The prognosis showed no significant difference between patients with T classification shifts and those with matching cT (c[m]T1a vs c[l]T1a: stratified log-rank test, $P = 0.17$; c[m]T1b vs c[l]T1b: stratified log-rank test, $P = 0.40$; Fig. 5). The corrected C-index was improved from 0.598 (95% CI 0.503–0.895) to 0.695 (95% CI 0.620–1.000) when using c(m)T to discriminate the prognosis of these patients. In addition, NRI and IDI analysis revealed that c(m)T showed a better performance for stratifying patient prognosis (NRI, 0.395; 95% CI -0.071 to 0.611; $P = 0.098$; IDI, 0.020; 95% CI -0.015 to 0.057; $P = 0.13$).

DISCUSSION

In our study, detecting the solid portion in the MW improved interobserver agreement on the SSNs classification from good to excellent, and the pathological malignancy could be estimated more precisely by measuring the solid portion in the MW. Importantly, our present study demonstrated that the clinical T classifications of patients with SSNs would shift when adopting the solid size measured in the MW. However, the performance of c(m)T for RFS prediction and stratification was equivalent to that of c(l)T for these patients.

An increasing number of SSNs have been detected because of the development of thin-section CT [14]. Recent studies have

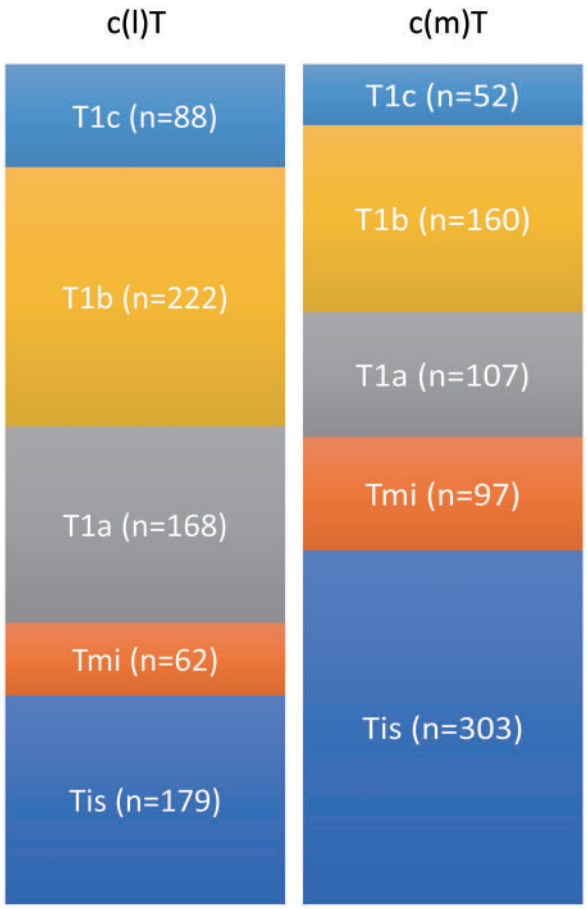

Figure 4: Distributions of clinical T classifications according to c(l)T and reclassifications by c(m)T. c(l)T: clinical T classifications according to the solid portion size measured with the lung window setting; c(m)T: clinical T classifications according to the solid portion size measured with the mediastinal window setting; cut-offs values were provided by the 8th edition T stage.

demonstrated that the solid portion of SSNs has a strong pathological correlation with invasive adenocarcinoma [6] and is more reflective of patient prognosis than the whole lesion size, including ground-glass opacity. Thus, the solid portion size of SSNs is currently used as a clinical T descriptor in the revised 8th edition of tumour, node and metastasis stage system [4]. In addition, the clinical T classifications proposed by the International Association for the Study of Lung Cancer and radiological lung nodule measurement guidelines by the Fleischer Society recommend that the solid portion of SSNs be measured via the LW of CT [4, 7], which employs a wide window width to display the lung parenchyma and its abnormal pathologies.

However, controversy remains in the usage of the LW for estimating the pathological invasiveness or survival outcomes for these patients. Tsutani *et al.* [15] reported that the solid portion size of PSNs measured in the LW was strongly related to pathological invasiveness. Similarly, our previous study indicated that the solid size measured in the LW acted as a predictive factor for RFS in clinical stage IA lung adenocarcinoma patients [16], which was also revealed in other studies [6, 17]. However, the usage of the MW has been advocated because of the unsatisfactory interobserver agreement on SSNs classifications and solid portion size measurements in the LW [8, 18].

It is widely acknowledged that measuring the solid portion size is not always easy due to the absence of global standards to distinguish between ground-glass opacity and solid components. However, SSNs could have a clear distinction from the background in the MW, and the nodule size and classifications were relatively easy to obtain. Therefore, the first important merit of the MW is excellent interobserver agreement on the SSNs classification. Van Riel*et al.* [9] reported a moderate interobserver agreement (kappa: 0.51) in the LW for 160 SSNs from the database of the Dutch-Belgian NELSON study. Ridge *et al.* [19] also reported moderate (kappa: 0.56) agreement among 6 thoracic radiologists on patient treatment because of the inconformity of the presence of solid components. Most of the disagreements were related to the presence or size of the solid component. In contrast, Revel *et al.* [8] revealed excellent interobserver agreement (kappa: 0.87) for nodule classification by using the MW in a series of 99 SSNs. Our present study indicated that the interobserver agreement on the nodule classifications was improved to 0.917 by using the MW. Another merit of the MW is that the consolidation size measured in the MW better predicted pathological invasiveness and malignancy [10, 20]. In contrast, our study revealed that the solid portion size measured in the MW better predicted pathological malignancy but failed to predict pathological invasiveness better. Considering that only 7 patients with lymph node metastasis and 39 patients with VPI were included in the analysis, a further validation cohort including a larger number of patients with pathological malignancy is needed.

To the best of our knowledge, however, only one study comparing the impact of LW and MW settings on clinical T classification and prognostic prediction is available, which analysed PSNs and pure solid nodules jointly [11]. Considering the favourable prognosis of ground-glass opacity [21], lung adenocarcinoma manifesting as PSNs should be defined as a special clinical subtype, and the effect of the MW on clinical T classifications for PSNs and pure solid nodules are recommended to be investigated separately [22]. Our study found out that the solid size of SSNs measured in the MW was mostly smaller than that measured in the LW and the clinical T classifications would inevitably shift. The first possible reason for this is that determining the boundary between a solid portion and its surroundings at the lower contrast of the LW may be difficult. The second possible reason is that the solid portion detected in the LW would disappear when applying the MW because of the more highly attenuated inner solid portion. Nevertheless, the 5-year RFS rate of pGGNs distinguished using different window settings was both 100%, and c(m)T and c(l)T were both independent prognostic indictors for patients with PSNs determined using the MW. The 5-year RFS rates showed no significant difference between the patients with shifting c(m)T and matching c(l)T classifications. Therefore, we presumed that the solid portion measured in the MW should be utilized considerably in the assessment of SSNs.

However, our study did not support the switching from the usage of the LW to the MW for the solid portion measurement. First, the solid portion size should be measured in a consistent manner using the LW at the present, and interobserver agreement on the nodule classifications using the LW was higher than 0.8. Apart from this, solid portion size measured in the LW had better performance in predicting pathological invasiveness, and the C-

Table 3: Univariable and multivariable Cox regression analyses for recurrence-free survival (RFS) in patients with 416 PSNs determined at the MW

Variables	Univariable		Multivariable			
			For c(l)T		For c(m)T	
	HR (95% CI)	*P*-value	HR (95% CI)	*P*-value	HR (95% CI)	*P*-value
Age (≥65 year)	1.395 (0.694–2.804)	0.35				
Sex (male)	1.652 (0.852–3.206)	0.14				
Lesion side (right)	0.797 (0.408–1.557)	0.51				
Presence of upstage	0.721 (0.099–5.272)	0.75				
Presence of downstage	0.617 (0.302–1.261)	0.19				
c(l)T		0.002		0.003		
Tmi/T1a	*Reference*		*Reference*			
T1b	2.399 (0.796–7.229)	0.12	3.379 (1.091–10.465)	0.035		
T1c	6.012 (2.010–17.985)	0.001	6.303 (2.102–18.898)	0.001		
c(m)T		0.001				0.005
Tmi/T1a	*Reference*				*Reference*	
T1b	2.542 (1.088–5.941)	0.031			3.304 (1.380–7.911)	0.007
T1c	5.354 (2.152–13.319)	<0.001			4.202 (1.671–10.565)	0.002
Surgery procedure (lobectomy)	1.045 (0.320–3.415)	0.94				
Histological subtype (LPA)	29.577 (13.290–65.823)	<0.001	32.327 (13.828–75.573)	<0.001	31.452 (13.005–76.066)	0.001
VPI (presence)	1.075 (0.329–3.513)	0.90				

Cut-off values were provided by 8th edition T stage.

c(l)T: clinical T classification determined using the lung window setting; c(m)T: clinical T classification determined using the mediastinal window setting; CI: confidence interval; HR: hazard ratio; LPA: lepidic-predominant adenocarcinoma; PSNs: part-solid nodules; VPI: visceral pleura infiltration.

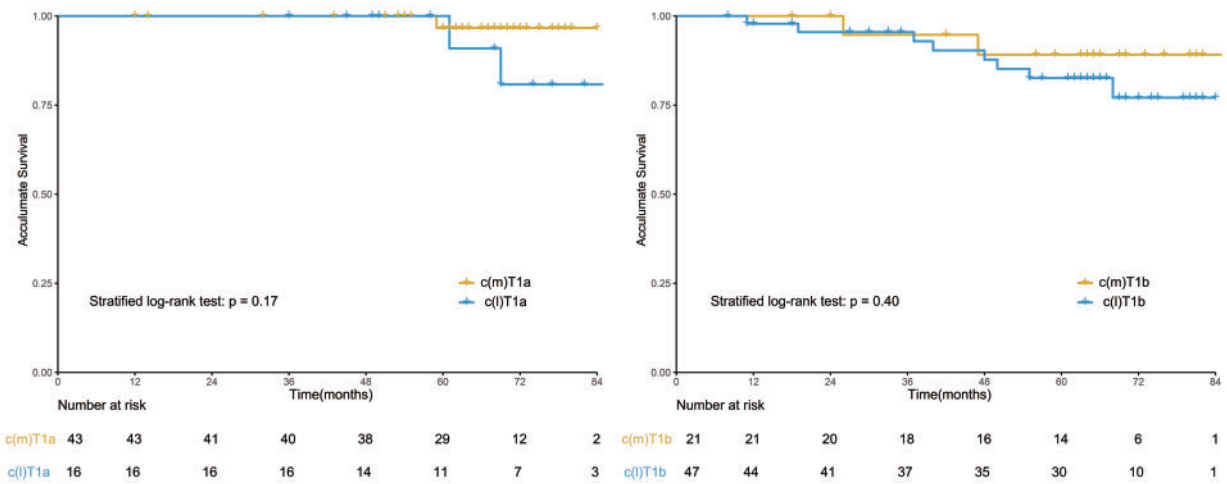

Figure 5: Kaplan–Meier survival curves for patients with T classifications shifts in the matched cohort. c(l)T1a and c(l)T1b: T classifications determined when applying the lung window setting; cut-offs were provided by the 8th edition T stage; c(m)T1a and c(m)T1b: T classifications shifts to T1a or T1b when applying the mediastinal window setting.

index analysis demonstrated that c(l)T provided better benefits for survival stratification than c(m)T. Accordingly, we deem it appropriate to adopt the LW for evaluating SSN following the established recommendation.

Limitations

There were several limitations in our study. First, only patients who underwent surgical resection were included in this study, which was not large number of patients with SSNs. However, a patient cohort with a definitive pathological diagnosis and follow-up information was preferred to investigate the prognosis of these patients. Second, 2 blinded radiologists with different levels of expertise were invited to review the CT scans and measure the solid portion size manually, which may result in bias. To minimize deviations, we applied the average solid portion size measured by 2 radiologists. Third, our study was retrospective and performed in a single centre; a multicentre validation cohort study may be needed to support our results.

CONCLUSION

In conclusion, applying the MW of CT showed no additional benefit for determining clinical T classification and evaluating prognosis in patients with SSNs. Therefore, it is appropriate to adopt the LW setting for SSN evaluations as per the current recommendations.

SUPPLEMENTARY MATERIAL

Supplementary material is available at *EJCTS* online.

Funding

This work was supported by Clinical Research Foundation of Shanghai Pulmonary Hospital (FK1936, FK1941, FK1942, FK1943) and Shanghai Municipal Health Commission (2018ZHYL0102, 2019SY072, 201940018).

Conflict of interest: none declared.

Author contributions

Mengmeng Zhao: Resources; Writing—original draft; Writing—review & editing. **Jiajun Deng:** Investigation; Writing—original draft; Writing—review & editing. **Tingting Wang:** Data curation. **Yingze Li:** Data curation. **Junqi Wu:** Data curation. **Yifang Zhong:** Data curation. **Xiwen Sun:** Software. **Gening Jiang:** Visualization. **Yunlang She:** Conceptualization; Investigation. **Yuming Zhu:** Supervision. **Dong Xie:** Supervision. **Chang Chen:** Conceptualization; Supervision.

Reviewer information

European Journal of Cardio-Thoracic Surgery thanks Luca Bertolaccini, Frank C. Detterbeck, Stefan B. Watzka and the other, anonymous reviewer(s) for their contribution to the peer review process of this article.

REFERENCES

[1] Hansell DM, Bankier AA, MacMahon H, McLoud TC, Muller NL, Remy J. Fleischner Society: glossary of terms for thoracic imaging. Radiology 2008;246:697–722.
[2] Lederlin M, Puderbach M, Muley T, Schnabel PA, Stenzinger A, Kauczor H-U *et al.* Correlation of radio- and histomorphological pattern of pulmonary adenocarcinoma. Eur Respir J 2013;41:943–51.
[3] Huang T, Lin K, Huang H, Chen Y, Ko K, Chang C *et al.* The role of the ground-glass opacity ratio in resected lung adenocarcinoma. Eur J Cardiothorac Surg 2018;54:229–34.
[4] Travis WD, Asamura H, Bankier AA, Beasley MB, Detterbeck F, Flieder DB *et al.* The IASLC Lung Cancer Staging Project: proposals for coding T categories for subsolid nodules and assessment of tumor size in part-solid tumors in the forthcoming eighth edition of the TNM Classification of Lung Cancer. J Thorac Oncol 2016;11:1204–23.
[5] Arenas-Jiménez J. Measurement of solid component in part-solid lesions with a mediastinal window setting? Radiology 2013;268:305–6.
[6] Lee KH, Goo JM, Park SJ, Wi JY, Chung DH, Go H *et al.* Correlation between the size of the solid component on thin-section CT and the invasive component on pathology in small lung adenocarcinomas manifesting as ground-glass nodules. J Thorac Oncol 2014;9:74–82.
[7] Bankier AA, MacMahon H, Goo JM, Rubin GD, Schaefer-Prokop CM, Naidich DP. Recommendations for measuring pulmonary nodules at CT: a statement from the Fleischner Society. Radiology 2017;285:584–600.
[8] Revel MP, Mannes I, Benzakoun J, Guinet C, Leger T, Grenier P *et al.* Subsolid lung nodule classification: a CT criterion for improving interobserver agreement. Radiology 2018;286:316–25.
[9] van Riel SJ, Sánchez CI, Bankier AA, Naidich DP, Verschakelen J, Scholten ET *et al.* Observer variability for classification of pulmonary nodules on low-dose CT images and its effect on nodule management. Radiology 2015;277:863–71.
[10] Samejima J, Ito H, Nakayama H, Nagashima T, Osawa J, Inafuku K *et al.* Which window setting is best for estimating pathologic invasive size and invasiveness? Ann Thorac Surg 2019;108:384–91.
[11] Kim H, Goo JM, Kim YT, Park CM. Clinical T categorization in stage IA lung adenocarcinomas: prognostic implications of CT display window settings for solid portion measurement. Eur Radiol 2019;29:6069–79.
[12] Machin D, Campbell MJ, Tan SB, Tan SH. Sample Size Tables for Clinical Studies, 2nd edn. Blackwell Science, 1997, 176–7. IBSN 0-86542-870-0.
[13] Landis JR, Koch GG. The measurement of observer agreement for categorical data. Biometrics 1977;33:159–74.
[14] Henschke CI, Yankelevitz DF, Mirtcheva R, Mcguinness G, Mccauley DI, Miettinen OS. CT screening for lung cancer: frequency and significance of part-solid and nonsolid nodules. AJR Am J Roentgenol 2002;178:1053–7.
[15] Tsutani Y, Miyata Y, Nakayama H, Okumura S, Adachi S, Yoshimura M *et al.* Prognostic significance of using solid versus whole tumor size on high-resolution computed tomography for predicting pathologic malignant grade of tumors in clinical stage IA lung adenocarcinoma: a multicenter study. J Thorac Cardiovasc Surg 2012;143:607–12.
[16] Su H, Dai C, She Y, Ren Y, Zhang L, Xie H *et al.* Which T descriptor is more predictive of recurrence after sublobar resection: whole tumour size versus solid component size? Eur J Cardiothorac Surg 2018;54:1028–36.
[17] Burt BM, Leung AN, Yanagawa M, Chen W, Groth SS, Hoang CD *et al.* Diameter of solid tumor component alone should be used to establish T stage in lung adenocarcinoma. Ann Surg Oncol 2015;22:1318–23.
[18] Haraguchi N, Satoh H, Kikuchi N, Kagohashi K, Ishikawa H, Ohtsuka M. Prognostic value of tumor disappearance rate on computed tomography in advanced-stage lung adenocarcinoma. Clin Lung Cancer 2007;8:327–30.
[19] Ridge CA, Yildirim A, Boiselle PM, Franquet T, Schaefer-Prokop CM, Tack D *et al.* Differentiating between subsolid and solid pulmonary nodules at CT: inter- and intraobserver agreement between experienced thoracic radiologists. Radiology 2016;278:888–96.
[20] Sakakura N, Inaba Y, Yatabe Y, Mizuno T, Kuroda H, Yoshimura K *et al.* Estimation of the pathological invasive size of pulmonary adenocarcinoma using high-resolution computed tomography of the chest: a consideration based on lung and mediastinal window settings. Lung Cancer 2016;95:51–6.
[21] Hattori A, Matsunaga T, Takamochi K, Oh S, Suzuki K. Importance of ground glass opacity component in clinical stage IA radiologic invasive lung cancer. Ann Thorac Surg 2017;104:313–20.
[22] Ye T, Deng L, Wang S, Xiang J, Zhang Y, Hu H *et al.* Lung adenocarcinomas manifesting as radiological part-solid nodules define a special clinical subtype. J Thorac Oncol 2019;14:617–27.